The Design of POD Considering Conventional and Renewable Power Generation

M. Mandour[1], M. EL-Shimy[2], F. Bendary[1] and W.M. Mansour[1]

[1]Electric Power and Machines Department – Benha University, Egypt. madel_ibec@yahoo.com

[2]Electric Power and Machines Department – Ain Shams University, Egypt. shimymb@gmail.com

Abstract— **FACTS devices employ high speed, and high power semi-conductor technologies to help better regulate the power systems. To improve the damping of oscillations in power systems, supplementary control laws can be applied to the existing FACTS devices. These supplementary actions are referred to as power oscillation damping (POD) control. In this paper, the POD controllers are designed using the frequency response method as a conventional design method. The POD will be designed in two test systems, the first one is a SMIB test system including conventional generation and series connected TCSC while the second system is a weakly interconnected power system including conventional and renewable wind power generation and shunt connected SVCs. In the weakly interconnected power system, the impact of wind power on the dynamic stability is considered and two situations are covered. The first one is the replacement of conventional power by wind power while the second one includes the addition of wind power to an existing conventional power generation system. The considered weakly interconnected power system is composed of two weakly interconnected areas. The objectives of wind power are to reduce the dependency between the two areas and the reduction of conventional fuel use while keeping acceptable damping levels. Two popular wind energy technologies are considered which are fixed speed SCIGs and the variable speed DFIGs. The results show that the wind power causes reduction in the damping of power system oscillations. Therefore, power oscillation damping controllers (POD) are integrated with the available SVCs. The modal analysis and the time-domain simulation are used for validating the POD efficient design.**

Index Terms— **FACTS, wind power, SCIG, DFIG, electromechanical oscillations, POD design, modal analysis, time domain simulation.**

I. INTRODUCTION

Power system stability has been recognized as an important problem for secure system operation since the 1920s [1]. The importance of this phenomenon has emerged due to the fact that many major blackouts in recent years caused by power system instability. As power systems have evolved through continuing growth in the interconnections and the increased operation in highly stressed conditions, different forms of power system instability have emerged.

FACTS technologies offer competitive solutions to today's power systems in terms of increased power flow transfer capability, enhancing continuous control over the voltage profile, improving system damping, minimizing losses, etc. FACTS technology consists of high power electronics based equipment with its real-time operating control.

The benefits of Flexible AC Transmission Systems (FACTS) devices are widely recognized by power system practitioners and the T&D community for enhancing both steady-state and dynamic performances of power systems [2-4]. The advent of these devices has required additional efforts in modeling and analysis, requiring engineers to have a wider background for a deeper understanding of power system's dynamic behavior.

The aim of this paper is to present procedures for designing power oscillation dampers (PODs) for FACTS devices in order to contextualize some important concepts of control theory into power system stability. A variety of design methods can be used for tuning POD parameters. The most common techniques are based on frequency response [5], pole placement [6], eigenvalues sensitivity [6, 7] and residue method [8].

POD design is presented in this paper using the frequency response method in two test systems which are the SMIB and the two area test system. The two area test system will include conventional and renewable wind generation. The competitive prices of wind energy place it as a major renewable energy resource [9, 10]. Egypt has many locations with excellent wind energy resources and large scale projects are already available [9 - 12]. In addition, future projects are currently in progress [12].

Based on the electrical topology, wind turbine generators (WTGs) can be grouped into two main categories [13 - 16]; fixed speed and variable speed WTGs. In comparison with the fixed speed technologies, the variable speed alternatives are known for their high aerodynamic efficiency, control capability, and stability.

Previous researches [17 - 19] show that the impact of wind power on the stability of power systems is highly

1962

related to the penetration level and the WTG technology. The higher the penetration level the significant the impact of wind power [18 - 20]. In fact, the dynamic behavior of a power system is largely determined by the behavior and interaction of the generators connecting to the power system. If wind turbines gradually start to replace the output of the synchronous generators, many aspects of the power system operation and control might be affected such as protection, frequency control, transient and voltage stability, among others [14, 15, 17 - 23].

Some studies have been applied to solve the power system stability problems associated with increasing penetration levels of renewable energy sources by the application of FACTS devices to enhance the dynamic and transient performance and improve the voltage stability of power systems which includes a large wind farm [24, 25].

The objectives of this paper include studying the impact of the wind power penetration in the two area test system on the small signal stability of power systems. In addition, high power system oscillations are mitigated by the proper design of power oscillation dampers (PODs) integrated with the available SVCs. The major types of WTG technologies are considered while two wind power scenarios are investigated. The first one is the replacement of conventional power by wind power while the second one is the addition of wind power to the generation capacity. The Kundur two-area system [26] is considered in this study due to its suitability for the analysis of complex dynamic phenomena as well as the availability of its data.

II. MODELING, AND MODAL ANALYSIS

A. Power system modelling and modal analysis

The power systems are dynamic systems that can be represented by differential algebraic equations in combination with non-linear algebraic equations. Hence, a power system can be dynamically described by a set of n first order nonlinear ordinary differential equations that are to be solved simultaneously. In vector-matrix notation, these equations are expressed as follows [26 - 28]:

$$\dot{x} = f(x, u) \qquad (1)$$
$$y = g(x, u) \qquad (2)$$

where: $x = [x_1, x_2 \cdots x_n]^t$, $u = [u_1, u_2 \cdots u_r]^t$,
$f = [f_1, f_2 \cdots f_n]^t$, $y = [y_1, y_2 \cdots y_m]^t$, $g = [g_1, g_2 \cdots g_m]^t$,
n is the order of the system, r is the number of inputs, and m is the number of outputs. The column vector x is called the state vector and its entries are the state variables. The vector u is the vector of inputs to the system, which are external signals that have an impact on the performance of the system. The output variables y are those that can be observed in the system. The column vector y is the system output vector and g is the vector of nonlinear functions defining the output variables in terms of state and input variables.

The design of POD controllers is based on linear system techniques. After solving the power flow problem, a modal analysis is carried out by computing the eigenvalues and the participation factors of the state matrix of the system. The dynamic system is put into state space form as a combination of coupled first order, linearized differential equations that take the form,

$$\Delta\dot{x} = A\Delta x + B\Delta u \qquad (3)$$
$$y = C\Delta x + D\Delta u \qquad (4)$$

where Δ represents a small deviation, A is the state matrix of size $n \times n$, B is the control matrix of size $n \times r$, C is the output matrix of size $m \times n$, and D is the feed forward matrix of size $m \times r$. The values of the matrix D define the proportion of input, which appears directly in the output.

The eigenvalues λ of the state matrix A can be determined by solving $\det[A - \lambda I] = 0$. If $\lambda_i = \sigma_i \pm j\omega_i$ denotes the ith eigenvalue of the state matrix A, then the real part gives the damping, and the imaginary part gives the frequency of oscillation. The relative damping ratio is then given by:

$$\xi_i = -\sigma_i / \sqrt{\sigma_i^2 + \omega_i^2} \qquad (5)$$

A damping ratio between 5% to 10% is acceptable for most power systems; however, the 10% value is recommended for secure system operation [27, 29].

If the state space matrix A has n distinct eigenvalues, then the diagonal matrix of the eigenvalues (Λ), the right eigenvectors (Φ), and the left eigenvectors (Ψ) are related by the following equations.

$$A\Phi = \Phi\Lambda \qquad (6)$$
$$\Psi A = \Lambda\Psi \qquad (7)$$
$$\Psi = \Phi^{-1} \qquad (8)$$

In order to modify a mode of oscillation by a feedback controller, the chosen input must excite the mode and it must also be visible in the chosen output. The measures of those two properties are the controllability and observability, respectively. The modal controllability ($\acute{B}$) and modal observability ($\acute{C}$) matrices are respectively defined by,

$$\acute{B} = \Phi^{-1}B \qquad (9)$$
$$\acute{C} = C\Phi \qquad (10)$$

The mode is uncontrollable if the corresponding row of the matrix $\acute{B}$ is zero. The mode is unobservable if the corresponding column of the matrix $\acute{C}$ is zero. If a mode is neither controllable nor observable, the feedback between the output and the input will have no effect on the mode.

The models of TCSC, SVC, SCIG and DFIG are described in [29 - 31].

B. The study systems

1. SMIB System:

The SMIB study system is shown in Fig.1. The system data are available at [26]. This system will be studied and analyzed with the aid of the *Power System Analysis Toolbox* (PSAT) version 2.1.7, the *Simulink* and the *control system toolbox* of Matlab 2012a [29, 30]. The PSAT model of the

1963

system is shown in Fig. 2. Based on [26], the study system consists of four 555 MVA, 24 kV, 60 HZ units supplying power to an infinite bus through two transmission circuits as shown in Fig.1. The four generators are represented by one equivalent generator that is represented by the second order dynamic model [26, 30]. On 2220 MVA and 24 kV base, the transient reactance of the equivalent generator (x'_d) is 0.3 p.u, its inertia constant (H) is 3.5 sec, and its damping coefficient (D) is 10 in p.u torque/p.u speed. The initial conditions of the system in p.u on the 2220 MVA, 24 KV base are $E_B = 0.995 \angle 0^o$, $E_t = 1.000 \angle 36^o$, $P = 0.9$, and $Q = 0.3$ (overexcited).
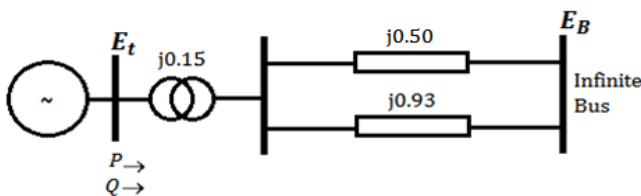
Fig. 1 The study system with the p.u network reactances are shown on 2220 MVA base
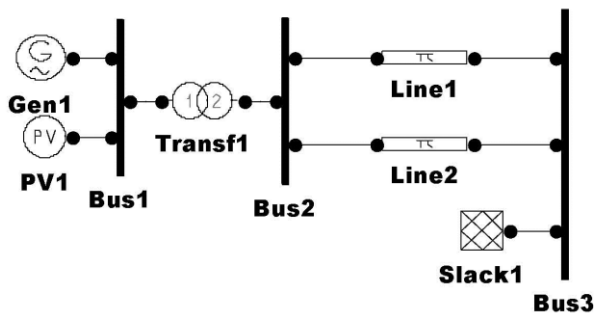

Fig. 2 The study system model in PSAT

In this test case, the constant admittance operation of the TCSC described in [29] will be considered for compensating differences between the reactances of two parallel transmission lines. The TCSC will be placed on line 2 shown in Fig. 2 and will be used to compensate the difference between the reactances of line 1 and line 2 of the study system shown in Fig. 1 and 2. The study system with the TCSC placed on line 2 is shown in Fig. 3. In this case, series compensation ratio is 0.462. The input variables to the PSAT block for modeling the TCSC are: $T_r = 0.01$ sec, $x_{cmin} = 0.36$ p.u, $x_{cmax} = 0.373$ p.u.
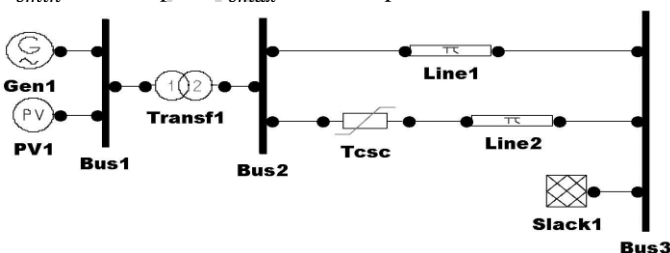

Fig.3 The study system after connecting the TCSC

2. The two area study system

The two area study system is shown in Fig.4. The system data are available at [26]. The original four-machine, two-area study system has been taken from [26] and has been modified by replacing the old fixed capacitors at buses 7 and 9 by SVCs as shown in Fig. 5 which also shows the PSAT Simulink model of the system. Each area consists of two synchronous generator units. The rating of each synchronous generator is 900 MVA and 20 kV. Each of the units is connected through transformers to the 230 kV transmission line. There is a power transfer of 400 MW from Area 1 to Area 2. The detailed base data, the line data, and the dynamic parameters for the machines, AVRs, PSS, and loads are given in [26].
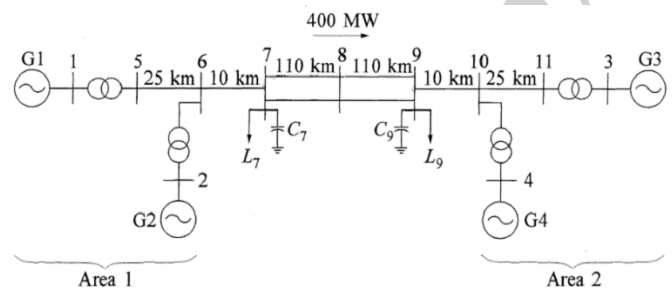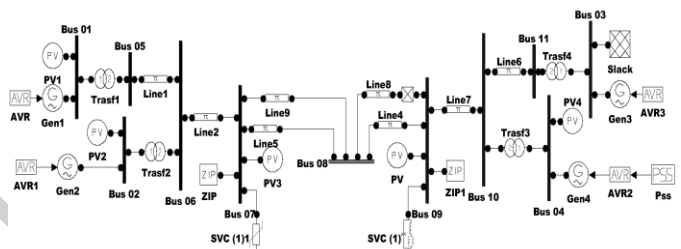

Fig. 4 The study system

Fig. 5 The study system model in PSAT

The wind power is included in the system considering two scenarios where two situations are considered in each scenario. A scenario is associated with the WTG technology while a situation is associated with the way at which the wind power is included. The first scenario considers the fixed-speed SCIG while the second one considers the variable-speed DFIG. For both scenarios the following situations are considered.

- *Situation 1*: the wind power will be used to replace a specific amount of the conventional generation in area 1. The objectives here are to reduce the ecological impact of the conventional generation and to reduce the dependency on fossil fuels.
- *Situation 2*: The wind power will be added to the conventional generation capacity available in area 2. The main objective in this case is to reduce the dependency of area 2 on area 1 i.e. the minimization of the power transfer over the weak tie-link.

As will be illustrated, the maximum or allowable amounts of wind power for both scenarios and both situations will be determined based on the modal analysis of the system. In addition, the PODs will be designed while the wind power is very close to its allowable limits.

III. POD DESIGN

1964

POD designs are presented in this paper using the frequency response method as a conventional method which is described in [27]. The main design objective is to achieve a predefined damping acceptable level of the electromechanical oscillations to improve the system performance. The general control diagram of the power system controlled by the POD is shown in Fig. 6 and 7. As shown in Fig. 7, the structure of the POD controller is similar to the classical power system stabilizer (PSS). The controller consists of a stabilizer gain, a washout filter, and phase compensator blocks. The gain Kw determines the amount of damping introduced by the POD and the phase compensator blocks provides the appropriate phase lead-lag compensation of the input signal.
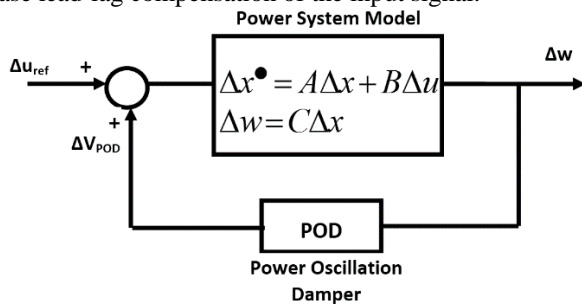
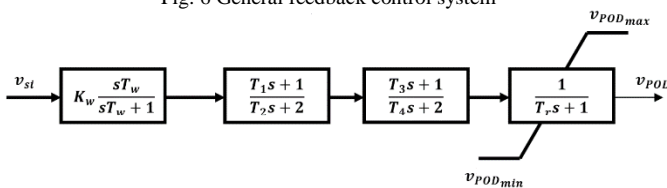**Power System Model**

Fig. 6 General feedback control system

Fig. 7: Scheme of the POD controller

The main design steps of the POD design using the frequency response method can be summarized as follows [27]:

1) Eigenvalue analysis: In this design, the critical modes of the uncompensated system (i.e. without the POD) are identified based on eigenvalues.
2) State-space form: In this step, all output and input matrices (A,B,C, and D) are determined.
3) Nyquist analysis: In this step, the value washout filter time constant is selected between 1 and 20 Sec then the Nuquist plot of the uncompensated loop including the washout filter is constructed. The required phase compensation φ is then determined from the constructed Nyquist plot. The objective is to obtain a good phase margin based on the critical frequency ω_n.
4) Compensator blocks tuning: Based on the value of φ that is determined in the previous step, the parameters of the phase compensator blocks are determined in this step using [27],

$$\alpha = \{1 - \sin(\varphi/m_c)\}/\{1 + \sin(\varphi/m_c)\} \quad (11)$$
$$T_2 = 1/\omega_n\sqrt{\alpha} \quad (12)$$
$$T_1 = \alpha T_2 \quad (13)$$

Where m_c is the number of the lead-lag blocks and ω_n is the frequency of the critical mode to be damped. The

value of m_c is usually one or two; Fig. 6 shows a POD with two lead-lag blocks (i.e. $m_c = 2$) which is considered in this paper. In this layout, T_3 and T_4 are equal to T_1 and T_2.

5) Damping ratio adjustment: In this step, the root locus plot of the compensated system is used to determine the value of Kw that provide an acceptable damping ratio (i.e. ξ ≥ 10%).

IV. RESULTS AND DISCUSSIONS

1. SMIB Test System :

The results will be presented through studying the system described in Fig.1 in three scenarios as shown in Fig.8. In the Time Domain Analysis (TDS), the considered small-signal disturbance is a +10 % step increase in the mechanical power input (P_m) to the equivalent generator of the study system shown in Fig. 2 and 3. The changes in the mechanical power will be started at t = 2 sec.
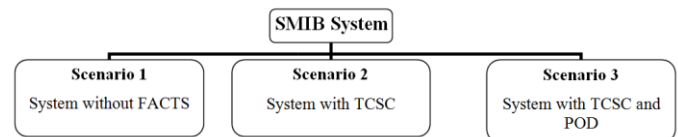

Fig.8 Study Scenarios

A) Impact of the TCSC on the small- signal stability

Tables I and II show the system eigenvalues and their participation factors of scenario 1 and scenario 2 respectively.

TABLE I
SCENARIO 1 - EIGENVALUES AND PARTICIPATION FACTORS

Eigenvalues	f (Hz)	ξ (%)	Participation factors		Most Associated States
			δ_1	ω_1	
-0.71429 ± j7.6085	1.2163	9.34	0.5	0.5	δ_1, ω_1

TABLE II
SCENARIO 2 - EIGENVALUES AND PARTICIPATION FACTORS

Eigenvalues	f (Hz)	ξ (%)	Participation Factors			Most associated states
			δ	ω	X_{1_TCSC}	
-0.71429±j8.0854	1.2919	8.79	0.5	0.5	0	δ, ω
-100	0	100%	0	0	1	$X_{1\ TCSC}$

It is clear from Tables I and II that both scenarios are stable; however, the eigenvalues of the system are changed as an effect of adding the TCSC to the system. The TCSC adds a non-oscillatory eigenvalue as depicted from Table II. The frequencies of the oscillatory modes of the system with TCSC are increased by 6.216% in comparison with the system without the TCSC while their damping ratios are reduced by 5.888%; (the percentage changes are calculated according to: % change = 100*(new value − old value)/old value). Therefore, the inclusion of the TCSC degrades the system stability. The damping ratio is less than 10%. Therefore, inclusion of POD is recommended to elevate the damping ratio to a value higher than or equal to 10%. POD

1965

design according to the frequency response is presented in the next section; the objective is to increase the damping ratio to an acceptable value i.e. $\xi \geq 10\%$. Various input signals to the POD will be considered.

B) Observability and controllability of various input signals

The observability and controllability of candidate feedback signals to the POD will be determined. Based on Fig. 2, these signals are the current across the transformer, the sending end active power, and the sending end reactive power. The modal controllability ($\acute{B}$) and modal observability ($\acute{C}$) matrices associated with the considered feedback signals are shown in Table III.

Table III
Modal observability and controllability of various feedback signals

Feedback signal	Modal observability C' matrix	Modal controllability B' matrix
The current across the transformer	$\begin{bmatrix} 1.3707 & 1.3707 & -0.2843 \end{bmatrix}$	$\begin{bmatrix} -0.08 - j0.93 \\ -0.08 + j0.93 \\ 100 \end{bmatrix}$
The sending end active power	$\begin{bmatrix} 1.223 & 1.223 & -0.2785 \end{bmatrix}$	
The sending end reactive power	$\begin{bmatrix} 0.1438 & 0.1438 & 0.0209 \end{bmatrix}$	

Considering the critical electromechanical modes shown in Table II (highlighted by gray shading), it is depicted from Table III that all the considered signals are observable and controllable. Highest observability is associated with the current across the transformer feedback signal followed by the sending end active power then the sending end reactive power. The POD design will be presented considering the current across the transformer as a feedback signal; however, the presented design algorithms are general and can be applied to design PODs considering any acceptable feedback signal.

C) POD designs

Designs with each of the considered feedback signals will be determined. The previous section completed the initial stages of the design i.e. building the input and output matrices, analysis of the eigenvalues, modal controllability, and modal observability. The washout filter time constant (T_w) can be arbitrary selected between 1 and 20 [32].

Optimum value of (T_w) can be selected based on a study that shows the impact of the washout filter (Tw) on the damping ratios and frequency of oscillation of the uncritical modes of the systems while keeping the critical ones at constant damping ratio (16% in this analysis). This is demonstrated in Fig.9.
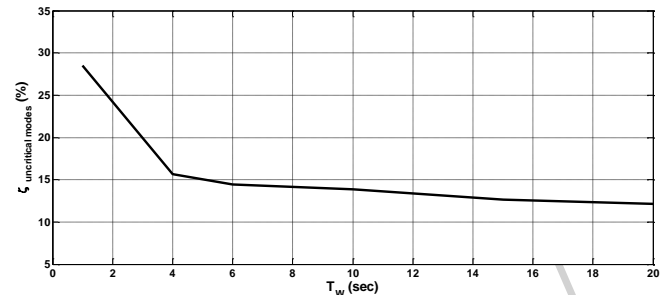

Fig.9 the effect of T_w on the damping ratios of the uncritical modes

Fig.9 shows that increasing Tw results in decreasing the damping ratios of some of the electromechanical modes that was originally not critical (i.e. their damping ratio was higher than 10%). Therefore, careful selection of T_w should be considered in the initial stages of the design. It is also important to know that a suitable value of T_w for a specific system may be not suitable for another system and it is clear from the previous analysis that in this system the optimum selection of (T_w) will be taken as 1.

With *the transformer current* as an input signal to the POD, the Nyquist plot (for positive frequencies) of the uncompensated OLTF (pre-design) and the compensated OLTF(post-design) is shown in Fig. 10.
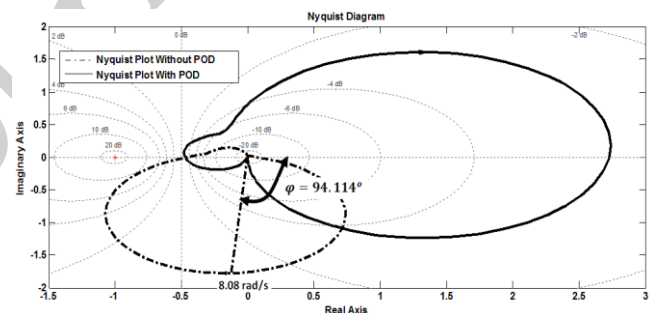

Fig. 10 Nyquist plots of SMIB system with and without POD

It is depicted from Fig. 10 and Table II that the OLTF for the system is stable, but presents poorly damped poles. For a good POD design, the resulting polar plot should be approximately symmetric with respect to the real axis of the complex plane [5, 32]. Based on the Nyquist plot shown in Fig. 10, the value of the angle φ required to relocate the critical frequency is 94.114°. Therefore, using equations (12) and (13), the parameters of the lead-lag compensators are T_1 = 0.3145 sec. and T_2 = 0.0487 sec. The gain K_w is determined based on the root locus of the system including the POD. The Matlab control system toolbox is used to construct the root locus as shown in Fig. 11. The gain K_w is determined by dragging the critical mode to an acceptable damping ratio which is chosen to be higher than 10%. As shown in Fig. 11, the value of the damping of the critical mode in the compensated system is set to 16% and the corresponding gain is 0.0786. The transfer function of the POD is then takes the form
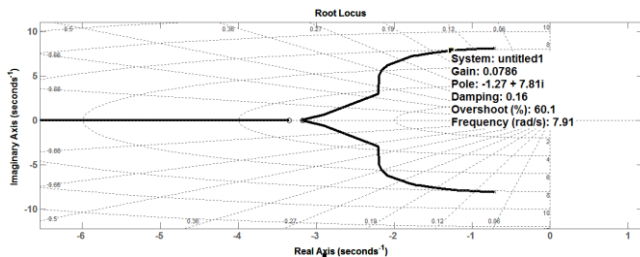
Fig. 11 Root locus of the compensated system and selection of the gain K_w

$$POD(s) = 0.0786 \left[\frac{s}{s+1}\right]\left[\frac{0.3147s+1}{0.0486s+1}\right]^2 \qquad (14)$$

With the POD connected to the system shown in Fig. 3 as shown in Fig. 12, the design will be evaluated by both the eigenvalue analysis and the TDS of the compensated system. The results of the eigenvalue analysis of the compensated system is shown in Table IV which indicates that the minimum damping of the system is improved to 15.97% as set by the POD design. Tables I and II show respectively that the damping of the system without TCSC is 9.34% and 8.79% in the uncompensated system with TCSC. This ensures the success of the POD design for improving the damping of the system.
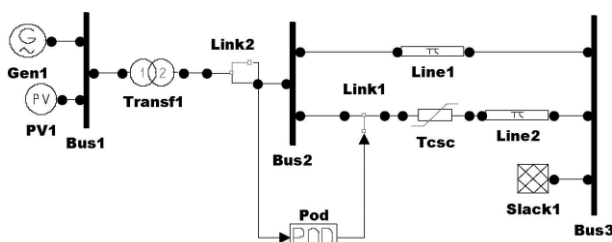

Fig.12 modelling of the SMIB in the 3rd scenario

TABLE IV
FREQUENCY RESONSE METHOD: EIGENVALUE ANALYSIS OF THE COMPENSATED SYSTEM
(Tw=1)

Eigenvalues	f (Hz)	ξ (%)	Most associated states
-16.992 ±j57.1679	9.4919	28.49%	X_{1_TCSC}, V_{2_POD}
-12.4811+j0	0	100%	V_{2_POD}
-1.2643±j7.8136	1.2597	15.97%	δ ,ω
-0.99877+j0	0	100%	V_{1_POD}

The TDS is performed considering a 10% step increase in the mechanical power input to the equivalent synchronous generator. This disturbance started at t = 2 sec. The simulation is performed using the Matlab control system toolbox. The responses of the systems of the three scenarios shown in Fig. 8 are compared as shown in Fig. 13.
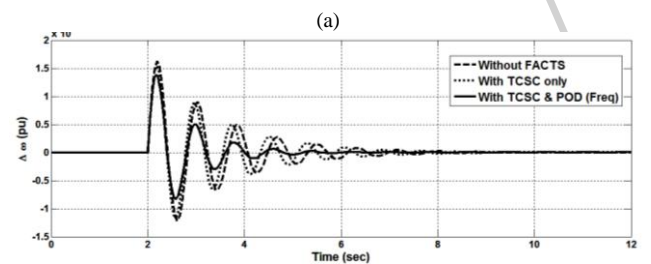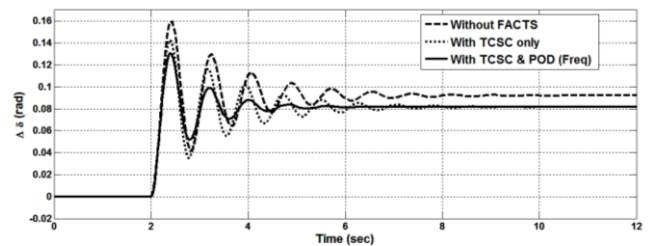

(a)

(b)

Fig. 13 TDS for 10% increase in the mechanical power: (a) Rotor angles; (b) Rotor angular speeds.

It is depicted from Fig. 13 that the POD improves the dynamic performance of the system through increasing the system damping, decreasing the overshoots, and decreasing the settling time.

Further Analysis:

In this section a summary of some other related results will be presented to show the effect of the POD input signal on damping of power system oscillations. The impact of POD input signal is shown in Fig. 14 which indicates that better dynamic performance can be achieved with the transformer reactive power as a feedback signal while the other feedback signals (i.e. the transformer current and the transformer active power) have the same impact on the dynamic performance of the system. Therefore, careful choice of the input signal is important for damping maximization through POD design. High damping can be achieved with the transformer reactive power as an input signal because of the less control loop stability restrictions on the POD parameters in comparison with other signals.
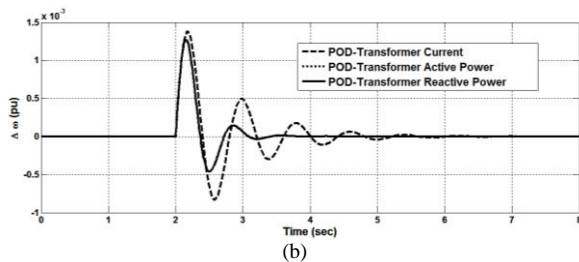

(a)

(b)
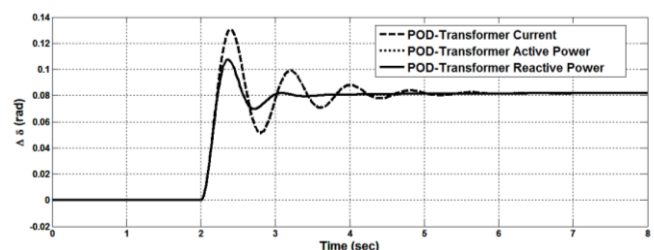
Fig. 14 TDS for 10% increase in the mechanical power with various
feedback signals: (a) Rotor angles; (b) Rotor angular speeds.

2. The Two Area Test System:

The results will be presented through studying the system described in Fig.15 considering the scenarios and situations explained in section II. The maximum wind penetration that can be replaced or added is determined based on the eigenvalues criteria. Near the maximum penetration point, POD will be designed using the frequency response method to improve the system dynamic performance when the system is subjected to a small disturbance (disconnection of line 8 for 100 msec after 1 sec operation in the initial steady state conditions). The data of the SCIG wind turbine can be found in [33] while the DFIG data are available at [34].

1) Scenario 1: SCIG:
A) Power Replacement

The SCIG will be added to area 1 on bus 12 as shown in Fig.5 for the purpose of replacing the generated power of synchronous generators by wind power till reaching the maximum wind penetration
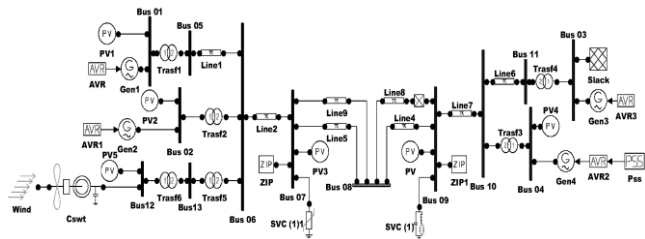

Fig.15 Two-area test system with SCIG added to Area 1 connected to bus 12

The eigenvalues with low damping ratios are shown in Table V. According to the results in Table V, The maximum generated power in area 1 that can be replaced by wind power equals 140 MW (10% of the total generated power by synchronous generators in Area 1) and after this value the system will be unstable as there is an existence of an eigenvalue located in the unstable region.

TABLE V
SCENARIO 1.A - DOMINANT EIGENVALUES AND PARTICIPATION

	Eigenvalues	f (Hz)	ξ (%)	Most associated states	Eigenvalue Status
$P_1+P_2=1260MW$ $P_{12}=140MW$	-0.59442±j6.5443	1.0458	9.04%	δ_2,ω_2	unacceptable
	-0.15025±j3.821	0.6086	3.9%	δ_3,ω_3	Critical
$P_1+P_2=1250MW$ $P_{12}=150MW$	-0.57982±j6.5303	1.0434	8.88%	δ_2,ω_2	unacceptable
	-0.14699±j3.8239	0.60903	3.86%	δ_3,ω_3	Critical
	-0.42722±j7.0026	1.1166	6.08%	omega_t_Cswt_1, gamma_Cswt	unacceptable
	0.12483+j0	0	-------	e1m_Cswt_1	+ve Eigenvalue

The POD is then designed near the maximum wind penetration point (P_{12}=140 MW) with the objective of increasing the damping ratios of the eigenvalues to an acceptable level. According to Table V, at P_{12} = 140 MW, there is a critical eigenvalue with damping ratio 3.9% and an unacceptable eigenvalue with damping ratio 9.04%. These damping ratios can be increased to acceptable levels (≥10%) by designing a POD. The sending current between Bus 5 and Bus 6 is used as a stabilizing signal to the POD. The POD gain (K_w) is selected based on the root-locus of the system as shown in Fig. 16. It is shown that with a again of 0.114 the 3.9% damping ratio becomes 23.88% while the 9.04% damping ratio becomes 10.7%. Therefore, this gain value results in acceptable damping ratios.
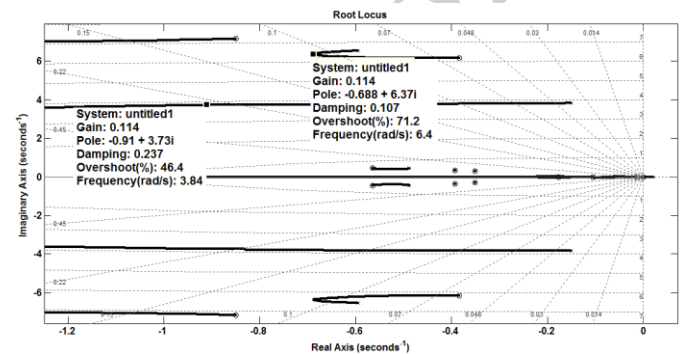

Fig. 16 Root locus of the compensated system and selection of
the gain *Kw* for Scenario 1.A

Using the frequency domain POD design method, the rest of the POD parameters are determined. The transfer function of the POD is, then takes the form

$$POD(s) = 0.114\left[\frac{s}{s+1}\right]\left[\frac{0.3186s+1}{0.215s+1}\right]^2 \quad (15)$$

With the POD connected to the system shown in Fig. 15 as shown in Fig. 17, the design will be evaluated by both the eigenvalue analysis and the TDS of the compensated system. The results of the eigenvalue analysis of the compensated system indicate that the minimum damping ratios of the critical and unacceptable eigenvalues are improved as desired to 23.88% & 10.7% respectively. This ensures the success of the POD design for improving the damping of the system.
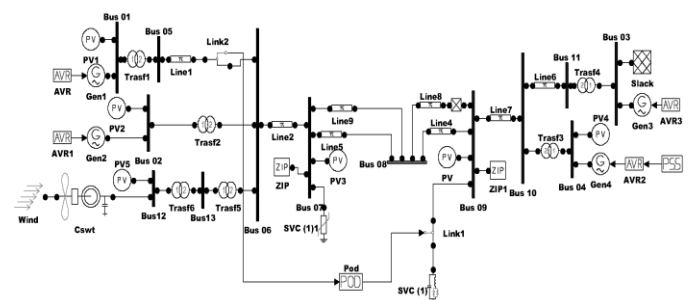

Fig.17 Two area test system with SCIG added to Area 1 and POD

The TDS is performed considering a disconnection of line 8 for 100 msec. This disturbance started at t = 1 sec. The

1968

simulation is performed using the Matlab control system toolbox. The responses of the system with and without POD are compared as shown in Fig. 18.
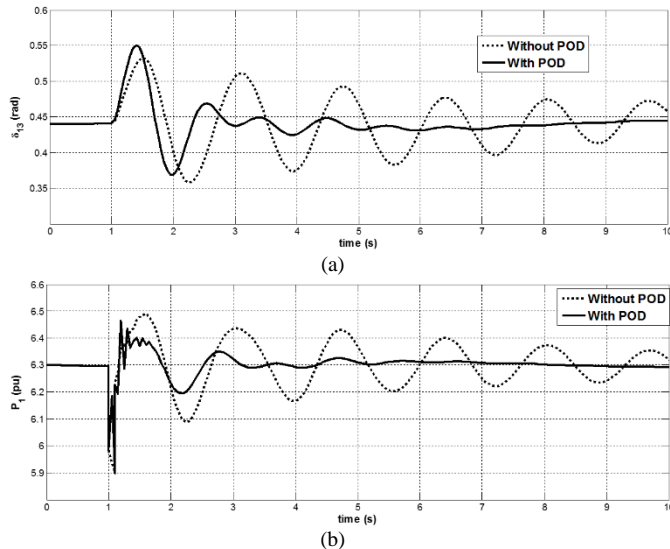

(a)

(b)

Fig. 18 TDS for 100msec disconnection of line8: (a) Rotor angle of G1; (b) Active power of G1.

It is depicted from Fig. 18 that the POD improves the dynamic performance of the system through increasing the system damping, and decreasing the settling time.

B) Power Addition:

The SCIG in this section will be added to area 2 on bus 12 for the purpose of reducing the power transfer from area 1 to area 2 by adding generated power by SCIG in area 2 till reaching the maximum wind penetration.

The eigenvalues with low damping ratios will be tabulated in Table VI as follow:

TABLE VI
SCENARIO 1.B - DOMINANT EIGENVALUES AND PARTICIPATION FACTORS

	Eigenvalues	f (Hz)	ξ (%)	Most associated states	Eigenvalue Status
P_{12}=140 MW	-0.59524±j6.5765	1.051	9.02%	δ_2,ω_2	unacceptable
	-0.17052±j3.9459	0.6286	4.31%	δ_3,ω_3	Critical
P_{12}=150 MW	-0.60136±j6.5699	1.05	9%	δ_2,ω_2	unacceptable
	-0.16879±j3.9522	0.62958	4.3%	δ_3,ω_3	Critical
	-0.57935±j6.9841	1.1154	8.28%	gamma_Cswt_1, e1m_Cswt_1	unacceptable
	0.17508+j0	0	-------	e1m_Cswt_1	+ve Eigenvalue

According to the results in Table VI, The maximum wind power that can be added to area 2 equals also to 140 MW and the system will be unstable when the generated power by SCIG equals 150 MW.

The POD is then designed near the maximum wind penetration point (P_{12}=140 MW) with the objective of increasing the damping ratios of the eigenvalues to an acceptable level. According to Table VI, at P_{12} = 140 MW, there is a critical eigenvalue with damping ratio 4.31% and an unacceptable eigenvalue with damping ratio 9.02%. These damping ratios can be increased to acceptable levels by designing a POD. The sending current between Bus 5 and

Bus 6 is used as a stabilizing signal to the POD. The POD gain (Kw) is selected based on the root-locus. For a gain of 0.062, the 4.31% damping ratio becomes 17.2% while the 9.02% damping ratio becomes 10.16%. Therefore, this gain value results in acceptable damping ratios.

In this case, the transfer function of the POD will take the form:

$$POD(s) = 0.062\left[\frac{s}{s+1}\right]\left[\frac{0.3097s+1}{0.2074s+1}\right]^2 \qquad (16)$$

With the POD connected to the system as shown in Fig. 19, the design will be evaluated by the eigenvalue analysis, which indicates that the minimum damping ratios of the critical and unacceptable eigenvalues are improved as desired to 17.23% & 10.16% respectively.
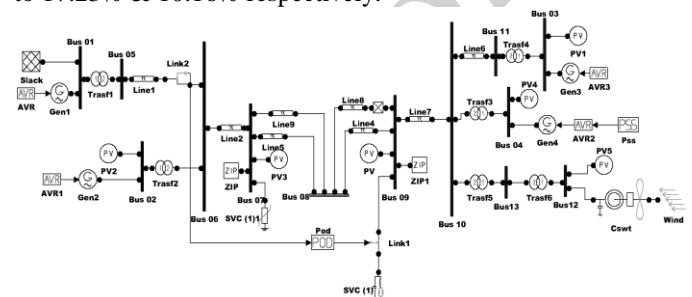

Fig.19 Two area test system with SCIG added to Area 2 and POD

The TDS of the compensated system is shown in Fig.20 considering the same disturbance to show the impact of POD on improving the damping of the system.
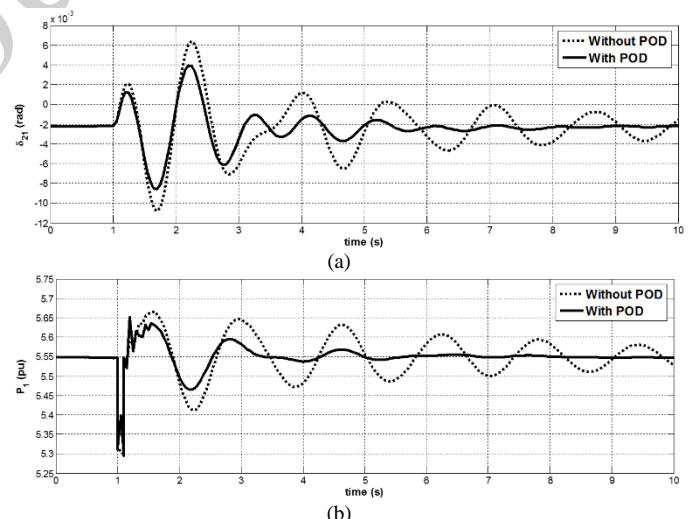

(a)

(b)

Fig. 20 TDS for 100msec disconnection of line8: (a) Rotor angle of G2; (b) Active power of G1.

2) Scenario 2 with DFIG:

A) Power Replacement:

The DFIG will be added to area 1 on bus 12 for the purpose of replacing the conventional power by wind power till reaching the maximum wind penetration

The eigenvalues with low damping ratios will be tabulated in Table VII as follow:

1969

TABLE VII
SCENARIO 2.A - DOMINANT EIGENVALUES AND PARTICIPATION FACTORS

	Eigenvalues	f (Hz)	ξ (%)	Most associated states	Eigenvalue Status
P₁+P₂=900MW P₁₂=500MW	-0.81087±j6.2776	1.0074	12.8%	δ₂ ,ω₂	acceptable
	-0.20784±j4.0177	0.64028	5.16%	δ₁ ,ω₁	Critical
P₁+P₂=850MW P₁₂=550MW	-0.85172±j6.2167	0.99866	13.5%	δ₂ ,ω₂	acceptable
	-0.22005±j4.0365	0.64339	5.4%	δ₁ ,ω₁	Critical
	-0.12055±j1.7216	0.27467	7.04%	δ₃ ,ω₃	unacceptable
	0.008 ±j0	0	------	omega_m_Dfig_1	+ve eigenvalue

According to the results in Table VII, The maximum generated power in area 1 that can be replaced by wind power equals 500 MW (35.7% of the total generated power by synchronous generators in Area 1) and after this value the system will be unstable.

The POD is then designed near the maximum wind penetration point (P_{12}=500 MW) with the objective of increasing the damping ratios of the eigenvalues to an acceptable level. According to Table VII, at P_{12} = 500 MW, there is a critical eigenvalue with damping ratio 5.16%. This damping ratio can be increased to an acceptable level by designing a POD. The sending current between Bus 5 and Bus 6 is used as a stabilizing signal to the POD. The POD gain (K_w) is selected based on the root-locus. For a gain of 0.0283, the 5.16% damping ratio becomes 10%. Therefore, this gain value results in acceptable damping ratio.
In this case, the transfer function of the POD will be as follow:

$$POD(s) = 0.0283 \left[\frac{s}{s+1}\right]\left[\frac{0.2871s+1}{0.2158s+1}\right]^2 \qquad (17)$$

With the POD connected to the system as shown in Fig. 21, the design will be evaluated by the eigenvalue analysis which indicates that the minimum damping ratios of the critical is improved as desired to 10%. The TDS of the compensated system is shown in Fig.22 to show the impact of POD on improving the damping of the system.
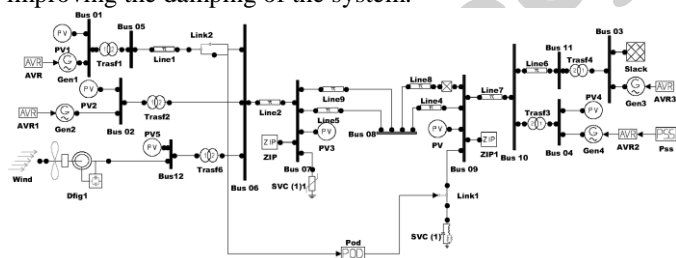

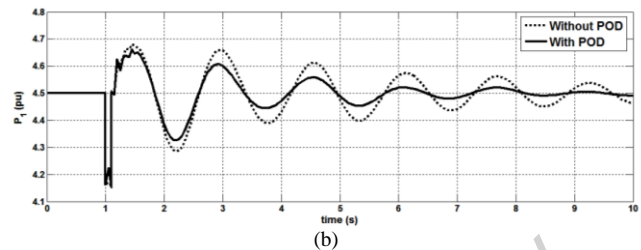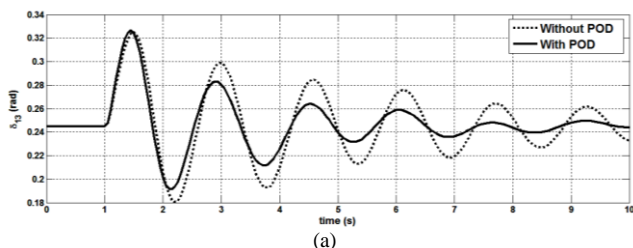Fig.21 Two area test system with DFIG added to Area 1 and POD

(a)

(b)
Fig. 22 TDS for 100msec disconnection of line8: (a) Rotor angle of G1; (b) Active power of G1.

B) Power Addition:

The DFIG in this section will be added to area 2 on bus 12 for the purpose of reducing the power transfer from area 1 to area 2 by adding generated power by DFIG in area 2 till reaching the maximum wind penetration. The eigenvalues with low damping ratios will be tabulated in Table VIII as follow:

TABLE VIII
SCENARIO 2.B - DOMINANT EIGENVALUES AND PARTICIPATION FACTORS

	Eigenvalues	f (Hz)	ξ (%)	Most associated states	Eigenvalue Status
P12= 350 MW	-0.78117±j6.3636	1.02	12.3%	δ₂ ,ω₂	acceptable
	-0.27893±j4.182	0.66	6.65%	δ₃ ,ω₃	Critical
P12= 400 MW	-0.83732±j6.2965	1.01	13.06%	δ₂ ,ω₂	acceptable
	-0.30421±j4.2103	0.67	7.1%	δ₃ ,ω₃	Critical
	-0.22003±j1.3624	0.21	16.6%	δ₁ ,ω₁	acceptable
	0.00074±j0	0	-----	omega_m_Dfig_1	+ve eigenvalue

According to the results in Table VIII, The maximum wind power that can be added to area 2 equals 350 MW and after this value the system will be unstable.

The POD is then designed near the maximum wind penetration point (P_{12}=350 MW) with the objective of increasing the damping ratios of the eigenvalues to an acceptable level. According to Table VIII, at P_{12} = 350 MW, there is a critical eigenvalue with damping ratio 6.65%. This damping ratio can be increased to an acceptable level by designing a POD. The sending current between Bus 5 and Bus 6 is used as a stabilizing signal to the POD. The POD gain (K_w) is selected based on the root-locus. For a gain of 0.03, the 6.65% damping ratio becomes 18%. Therefore, this gain value results in acceptable damping ratio.
The transfer function of the POD will take the form:

$$POD(s) = 0.03 \left[\frac{s}{s+1}\right]\left[\frac{0.3365s+1}{0.1699s+1}\right]^2 \qquad (18)$$

With the POD connected to the system as shown in Fig. 23, the design will be evaluated by the eigenvalue analysis, which indicates that the minimum damping ratios of the critical is improved as desired to 18%. The TDS of the compensated system is shown in Fig.24 to show the impact of POD on improving the damping of the system.
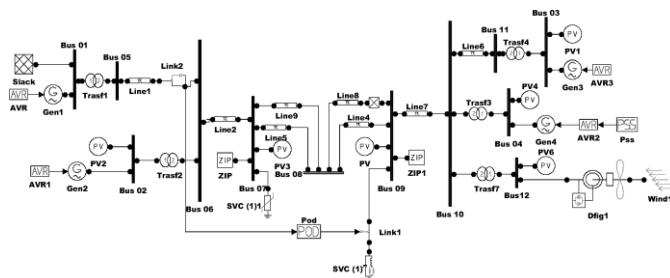
1970

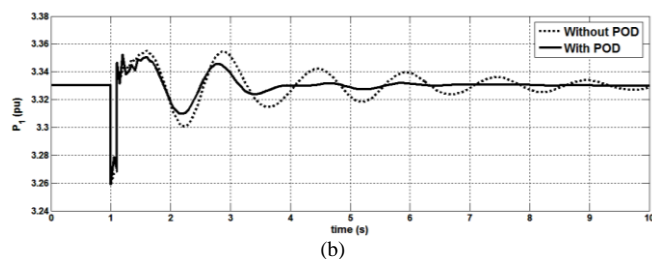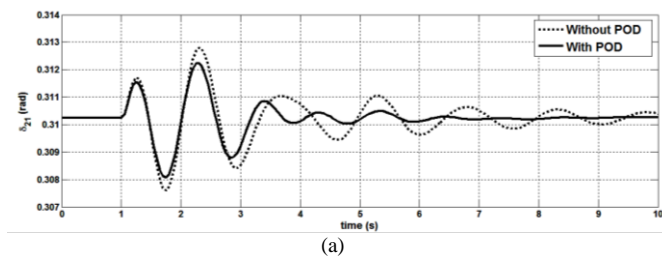Fig.23 Two area test system with DFIG added to Area 2 and POD

(a)

(b)

Fig. 24 TDS for 100msec disconnection of line8: (a) Rotor angle of G2; (b) Active power of G1.

V. CONCLUSIONS

POD is presented in this paper for improving the damping and stability of power systems. a popular method has been used for control design and successfully implemented for determining the parameters of POD. The method is the frequency domain method. The modal analysis as well as the time domain simulation verifies the results and show the dynamical benefits gained from the POD. In addition, critical design issues such as selection of the POD input signal and value of the time constant of the washout filter are also summarized in the SMIB study system.

The POD has been designed in the two area test system which includes FACTS-SVCs and two types of WTGs which are SCIG and DFIG. The design steps of POD have been achieved near the maximum penetration points which have been evaluated using the eigenvalues criteria.

Results show that the maximum wind penetration of the power system, including DFIG is more than that which includes SCIG. The POD in all cases provides an effective mean to enhance the small signal stability of the power system which is subjected to small disturbance. The results were confirmed by both the eigenvalues and time domain simulation.

REFERENCES

[1] P. Kundur, V. Ajjarapu, G. Andersson, A. Bose, C. Canizares, N. Hatziargyriou, D. Hill, A. Stankovic, C. Taylor, T. V. Cutsem and V. Vittal, "Definition and classification of power system stability ieee/cigre joint task force on stability terms and definitions", IEEE Transactions on Power Systems, Vol.19, No.3, Aug. 2004.

[2] J. J. Paserba, "How FACTS controllers benefit AC transmission systems," presented at the IEEE Power Engineering Society General Meeting, Denver, CO, 2004.

[3] Y. H. Song and A. T. Johns, Flexible AC Transmission Systems (FACTS). London: The Institution of Electrical Engineers, 1999.

[4] N. G. Hingorani and L. Gyugyi, Understanding FACTS: Concepts and Technology of Flexible AC Transmission Systems. New York: Institute of Electrical and Electronics Engineers, 2000.

[5] N. Martins and L. Lima, "Eigenvalue and Frequency Domain Analysis of Small-Signal Electromechanical Stability Problems," IEEE Symposium on Application of Eigenanalysis and Frequency Domain Method for System Dynamic Performance, 1989.

[6] B. C. Pal, "Robust pole placement versus root-locus approach in the context of damping interarea oscillations in power systems," IEE Proceedings on Generation, Transmission and Distribution, vol. 149, Nov 2002.

[7] R. Rouco and F. L. Pagola, "An eigenvalue sensitivity approach to location and controller design of controllable series capacitors for damping power system oscillations," IEEE Transactions on Power Systems, vol. 12, Nov 1997.

[8] R. Sadikovic, et al., "Application of FACTS devices for damping of power system oscillations," presented at the IEEE Power Tech, St. Petersburg, Russia, June 2005.

[9] M. EL-Shimy. "Optimal site matching of wind turbine generator: case study of the Gulf of Suez region in Egypt," Renewable Energy, Vol. 35, No. 8, 2010, pp. 1870-1878.

[10] Saad Chakkor, Mostafa Baghouri and Hajraoui Abderrahmane, "On-line Wind Turbine Remote Monitoring and Fault Detection Based on Intelligent Device", International Electrical Engineering Journal(IEEJ), Vol. 5, No.8, 2014, pp. 1495-1502.

[11] M. EL-Shimy. "Adequacy-Based Placement of WECS in Egypt," presented at the MEPCON'08 IEEE International Conference, Aswan, Egypt, 2008.

[12] New & Renewable Energy Authority (NREA) of Egypt. Available: http://nrea.gov.eg/english1.html

[13] M. EL-Shimy, "Probable Power Production in Optimally Matched Wind Power Systems," International journal of Sustainable Energy Technologies and Assessments (SETA).2, pp. 55–66, 2013.

[14] M. EL-Shimy, "Wind Energy Conversion Systems: Reliability Prospective," *Encyclopedia of Energy Engineering and Technology,* vol. 2, pp. 2184 - 2206, 2014.

[15] M. EL-Shimy and N. Ghaly, "Grid-Connected Wind Energy Conversion Systems: Transient Response," Taylor & Francis - Encyclopedia of Energy Engineering and Technology, CRC Press, 2014.

[16] R. Zavadil, N. Miller, A. Ellis and E. Muljadi., "Queuing up," Power and Energy Magazine, IEEE, vol. 5, pp. 47-58, Nov.-Dec 2007.

[17] J. Slootweg and W. Kling, "The impact of large scale wind power generation on power system oscillations," Electric Power Systems Research, vol. 67, pp. 9-20, October 2003.

[18] EL-Shimy M, Badr MAL, Rassem OM. Impact of Large Scale Wind Power on Power System Stability. MEPCON'08 IEEE International Conference; 12 – 15 March 2008; Aswan, Egypt, 2008. p. 630 – 636.

[19] P. Ledesma and C. Gallardo, "Contribution of variable-speed wind farms to damping of power system oscillations," presented at the Power Tech, 2007 IEEE Lausanne, Lausanne, 2007.

[20] N. Ghaly, M. EL-Shimy, M. Abdelhamed, "Consistence of Wind Power Technologies with the Fault Ride-through Capability Requirements," presented at the MEPCON'14 IEEE International Conference, Cairo, Egypt, 2014.

1971

[21] Z. Chen, "Issues of connecting wind farms into power systems," presented at the Transmission and Distribution Conference and Exhibition: Asia and Pacific, 2005 IEEE/PES, Dalian, 2005.

[22] M. EL-Shimy, "Modeling and analysis of reactive power in grid-connected onshore and offshore DFIG-based wind farms," *Wind Energy,* vol. 17, no. 2, pp. 279–295, 2014

[23] M. Ahmed, M. EL-Shimy, and M. Badr, "Advanced modeling and analysis of the loading capability limits of doubly-fed induction generators," Sustainable Energy Technologies and Assessments, vol. 7, pp. 79-90, 2014.

[24] W. Qiao, Harley, R.G. and Venayagamoorthy, G.K., "Effects of FACTS Devices on a Power System Which Includes a Large Wind Farm," presented at the Power Systems Conference and Exposition, 2006. PSCE '06. 2006 IEEE PES, Atlanta, GA, 2006.

[25] M. Fazli, A.R. Shafighi, A. Fazli and H.A. Shayanfar, "Effects of STATCOM on wind turbines equipped with DFIGs during grid faults," presented at the World Non-Grid-Connected Wind Power and Energy Conference (WNWEC), Nanjing, 2010

[26] P. Kundur, "Power system stability and control", New York: McGrew Hill, (1994).

[27] M. Mandour, M. EL-Shimy, F. Bendary, and W.M.Mansour , "Damping of Power Systems Oscillations using FACTS Power Oscillation Damper – Design and Performance Analysis", MEPCON'14 IEEE International Conference; Dec. 23 – 15, 2014, Cairo, Egypt, 2014.

[28] C. E. Ugalde-Loo, et al., "Multi-machine power system state-space modelling for small-signal stability assessments," Applied Mathematical Modelling, vol. 37, pp. 10141-10161, 15 December 2013.

[29] F. Milano, Power System Analysis Toolbox – Documentation for PSAT Version 2.0.0, Feb 2008.

[30] F. Milano. PSAT version 2.1.7 Available: http://www3.uclm.es/profesorado/federico.milano/psat.htm.

[31] F. Milano, "An Open Source Power System Analysis Toolbox" IEEE Transactions on Power Systems," IEEE Transactions on Power Systems, vol. 20, Aug 2005.

[32] H. M. Ayres, I. Kopcak, M. S. Castro, F. Milano and V. F. d. Costa, "A didactic procedure for designing power oscillation damper of facts devices", Simulation Modelling Practice and Theory, vol.18, no.6 June 2010.

[33] J. C. Munoz and C. A. Canizares, "Comparative stability analysis of DFIG-based wind farms and conventional synchronous generators," presented at the Power Systems Conference and Exposition (PSCE), 2011 IEEE/PES, Phoenix, AZ, 2011.

[34] B. Mehta, et al., "Small signal stability analysis of power systems with DFIG based wind power penetration," International Journal of Electrical Power & Energy Systems, vol. 58, pp. 64-74, June 2014.